Retrosynthesis of Nacre via Amorphous Precursor Particles

Nicole Gehrke,[†] Nadine Nassif,[†] Nicola Pinna,[§] Markus Antonietti,[†] Himadri S. Gupta,[‡] and Helmut Cölfen*,[†]

Colloid Chemistry and Biomaterials, Max-Planck-Institute of Colloids and Interfaces, Research Campus Golm, D-14424 Potsdam, Germany, and Institut für Anorganische Chemie, Martin-Luther-Universität Halle-Wittenberg, Kurt-Mothes-Strasse 2, 06120 Halle (Saale), Germany

Received September 26, 2005
Revised Manuscript Received November 15, 2005

Biominerals came into the focus of researchers due to their hierarchical organization and superior material properties. Thus, understanding of their formation processes is an important issue in materials chemistry but is still far from being achieved. Biominerals are hybrid materials consisting from a mineral and an organic part—the organic matrix, usually subdivided into the soluble and insoluble fraction. Nacre is a frequently investigated[1−7] and copied[8−11] biomineral system. A commonly used method to learn about biomineral formation processes is the crystallization of a mineral phase in the presence of particular proteins from the soluble organic matrix,[12−14] whereas the insoluble matrix was rarely used as such.[15,16]

Herein we report a retrosynthetic approach toward artificial nacre as a biomineral model system. For the first time, synthetic nacre morphologically indistinguishable from the natural archetype could be prepared.

Our approach is 2-fold. First, we used the insoluble organic nacre matrix of the shell of *Haliotis laevigata* as a confined reaction environment, as in nature the mineralization takes place in the preformed matrix.[17,18] It is expected that the insoluble matrix defines the hybrid microstructure and outer shape by its sheer geometrical presence. Second, we provide calcium and carbonate not in the form of ions but as amorphous intermediate nanoparticles as found, for example, in sea urchin spines.[19] One might think that these precursors can easily allow for high mass fluxes and increase of crystallization speed, independent of ion products, pH, and osmotic forces, which are to be balanced for biological operations. Moreover, they are regarded as key intermediates in a variety of in vitro crystallization reactions.[20,21] Therefore, we regard the pathway via amorphous nanoparticles as ideally suited to mimic biomineralization. We employ a simple synthetic polymer (polyaspartic acid) as an additive for their intermediary stabilization and do not use specific soluble proteins. By such an approach, we learn more about the mechanisms of biomineralization, particularly the role of the soluble and insoluble matrix.

Original nacre consists of a layered arrangement of pseudo-hexagonally shaped, nearly single crystalline aragonite (calcium carbonate) platelets[5] with a diameter of about 10−15 μm and a thickness of about 500 nm.[18] They are elongated along their *a*- and *b*-axes and expose their (001) faces toward the approximately 50 nm thick insoluble organic matrix,[1] which is described as a sandwich-like structure of a fibrous chitin core between two (insoluble) protein layers.[1,17]

Artificial nacre was synthesized by remineralization of the insoluble matrix of natural nacre (*H. laevigata*) after demineralization and removement of soluble proteins with 10% acetic acid (4 d at room temperature and solvent exchange) via the gas diffusion method.[22] Matrix pieces were placed in 20 mL of calcium chloride solution (10 mM) containing polyaspartic acid (Aldrich, 6000 g/mol) in the concentration range of micrograms per milliliter.[23] Two flasks, containing the solution with the matrix and 1 g of ammoniumcarbonate, respectively, were covered with punched Parafilm and placed into a closed chamber (1000 cm^3) for 24 h at room temperature. Afterward, the matrix pieces were removed from solution, washed with water, and dried.

The artificial nacre (Supporting Information Figure 1a) obtained here after only 24 h resembles closely the natural nacre (Supporting Information Figure 1b), as shown for fracture surfaces by scanning electron microscopy (SEM).

Investigation of synthetic nacre with transmission electron microscopy (TEM) reveals areas with different degrees of

* Corresponding author. Tel: +49-331-567-9513. Fax: +49-331-567-9502. E-mail: coelfen@mpikg.mpg.de.
[†] Colloid Chemistry, Max-Planck-Institute of Colloids and Interfaces.
[‡] Biomaterials, Max-Planck-Institute of Colloids and Interfaces.
[§] Martin-Luther-Universität Halle-Wittenberg.

(1) Nakahara, H. In *Biomineralization and Biological Metal Accumulation*; Westbroek, P., de Jong, E. W., Eds.; D. Reidel: Dordrecht, The Netherlands, 1983; pp 225−230.
(2) Marin, F.; Gilles, L. *C. R. Palevol* **2004**, *3*, 469.
(3) Levi-Kalisman, Y.; Falini, G.; Addadi, L.; Weiner, S. *J. Struct. Biol.* **2001**, *135*, 8.
(4) Weiner, S.; Traub, W. *Philos. Trans. R. Soc. London, Ser. B* **1984**, *304*, 452.
(5) Zaremba, C. M.; Belcher, A. M.; Fritz, M.; Li, Y.; Mann, S.; Hansma, P. K.; Morse, D. E.; Speck, J. S.; Stucky, G. D. *Chem. Mater.* **1996**, *8*, 679.
(6) Fritz, M.; Belcher, A. M.; Radmacher, M.; Deron, A. W.; Hansma, P. K.; Stucky, G. D.; Morse, D. E.; Mann, S. *Nature* **1994**, *371*, 49.
(7) Lin, A.; Meyers, M. A. *Mater. Sci. Eng.* **2005**, *A390*, 27.
(8) Lee, J. S.; Lee, Y. J.; Tae, E. L.; Park, Y. S.; Yoon, K. B. *Science* **2003**, *301*, 818.
(9) Sellinger, A.; Weiss, P. M.; Nguyen, A.; Lu, Y.; Assink, R. A.; Gong, W.; Brinker, C. J. *Nature* **1998**, *394*, 256.
(10) Tang, Z.; Kotov, N. A.; Maganov, S.; Ozturk, B. *Nat. Mater.* **2003**, *21*, 413.
(11) Volkmer, D.; Harms, M.; Gower, L.; Ziegler, A. *Angew. Chem., Int. Ed.* **2005**, *44*, 639.
(12) Falini, G.; Albeck, S.; Weiner, S.; Addadi, L. *Science* **1996**, *271*, 67.
(13) Belcher, A. M.; Wu, X. H.; Christensen, R. J.; Hansma, P. K.; Stucky, G. D.; Morse, D. E. *Nature* **1996**, *381*, 56.
(14) Wheeler, A. P.; George, J. W.; Evans, C. A. *Science* **1981**, *212*, 1397.
(15) Watabe, N.; Bernhardt, A. M.; Kingsley, R. J.; Wilbur, K. M. *Trans. Am. Microsc. Soc.* **1986**, *105*, 311.
(16) Watabe, N.; Wilbur, K. M. *Nature* **1960**, *188*, 334.
(17) Weiner, S.; Addadi, L. *J. Mater. Chem.* **1997**, *7*, 689.
(18) Nakahara, H. *Venus* **1979**, *38*, 205.
(19) Politi, Y.; Arad, T.; Klein, E.; Weiner, S.; Adadi, L. *Science* **2004**, *306*, 1161.
(20) Addadi, L.; Raz, S.; Weiner, S. *Adv. Mater.* **2003**, *15*, 959.
(21) Cölfen, H.; Mann, S. *Angew. Chem., Int. Ed.* **2003**, *42*, 2350.
(22) Addadi, L.; Moradian, J.; Shay, E.; Maroudas, N. G.; Weiner, S. *Proc. Natl. Acad. Sci. U.S.A.* **1987**, *84*, 2732.
(23) Olszta, M. J.; Douglas, E. P.; Gower, L. B. *Calcif. Tissue Int.* **2003**, *72*, 583.

10.1021/cm052150k CCC: $30.25
Published on Web 12/03/2005

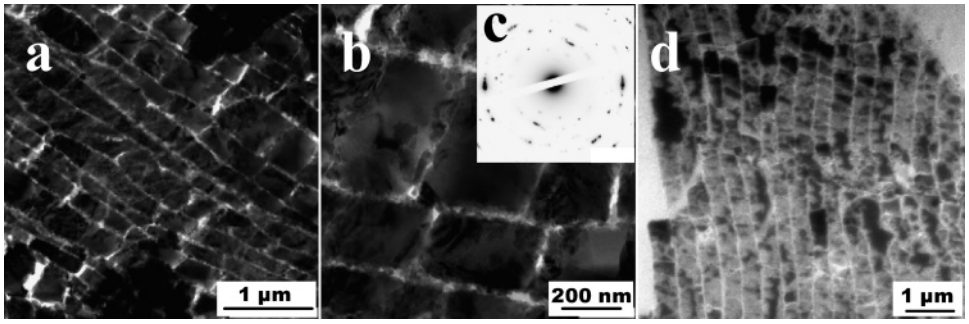

Figure 1. TEM micrographs of (a and b) of highly mineralized parts of synthetic nacre after 24 h reaction time. (c) Electron diffraction pattern of the platelets in panel b. (d) Original nacre from *Haliotis laevigata*.

mineralization. Highly mineralized areas bear platelets of 100−400 nm thickness and up to 1.6 μm width showing a variation in the platelet width (Figure 1a,b) due to unevenly spaced nucleation centers. The platelet thickness is in part lower than in the natural archetype due to partial collapse of the demineralized matrix during its preparation and handling. Electron diffraction taken from few platelets in a remineralized zone shows that they are not all oriented along the same direction, as they do not provide a single crystalline diffraction pattern (Figure 1c). The *d*-spacing determined from the electron diffraction corresponds to pure calcite. This is confirmed by infrared spectroscopy of the remineralized sample showing the characteristic peaks of calcite (Supporting Information Figure 2).

These platelets are divided by bright layers of organic matrix with lower electron density, very similar to TEM micrographs of original nacre (Figure 1d). The two major differences are a calcitic mineral phase (instead of aragonite) and smaller lateral dimensions of the primary platelets, indicating a higher nucleation rate on the demineralized tissue surface compared to its natural state. This is presumably due to the fact that aragonite nucleating moieties are potentially degraded during the acidic demineralization or absent (soluble proteins).[12,24]

Low mineralized areas of the samples reveal information about the formation of these platelets. TEM pictures of both the completely demineralized (Figure 2a) as well as the remineralized matrix in regions with low mineralization (Figure 2b) depict the organic layers being separated from each other by distances up to approximately 400 nm, indicating that the matrix does not collapse but scaffolds the mineralization reaction.

Figure 2, panels b and c, shows aggregates of different size and shape composed of the primary nanoparticles (of about 30 nm in size) in contact with the layers. These aggregates consist of calcite, as shown by electron diffraction (Figure 2e).

As amorphous precursor particles are created in the excess solution phase (as described by Olszta et al.[23] and proven here by electron diffraction, Supporting Information Figure 3b), it is to be concluded that they migrate into the demineralized matrix to transform into the observed platelets.

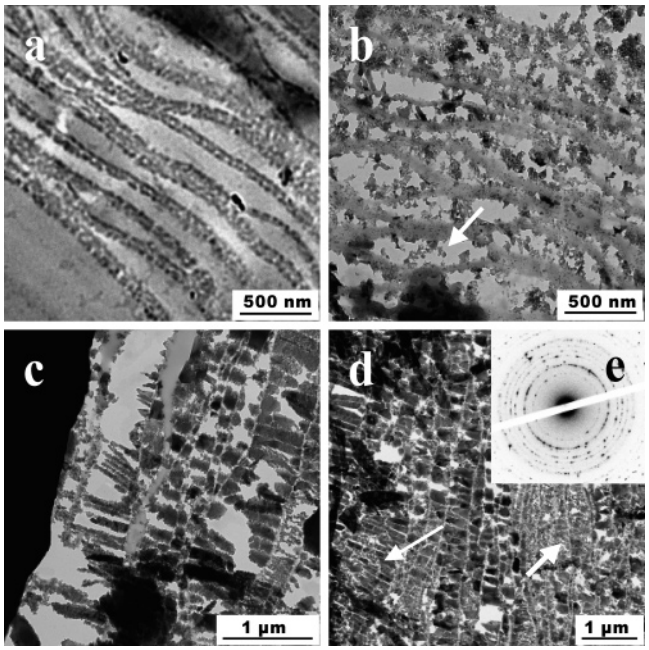

Figure 2. TEM pictures of completely demineralized matrix (a). (b−d) Matrix after 24 h remineralization: (b) area with low mineralization degree containing nanoparticles (ca. 30 nm) starting to form aggregates; (c) area with higher mineralization degree showing aggregates; (d) highly mineralized area, platelets (see Figure 1a,b) as well as aggregates observable. (e) Electron diffraction pattern of the aggregates in panel d. The sample in panel a was critical point-dried; samples in panel b−d were prepared as described above.

This follows previous work in which a collagen matrix was mineralized via amorphous precursor particles.[23] In our experiments nanoparticles are found throughout the tissue (Figure 2b, arrow) demonstrating that they can pass the micron-sized matrix structure, probably via 5−50 nm sized pores,[25] and can enter from the outer rim. The precursor particles attach to the matrix, aggregate, and grow from the tissue (Figure 2b,c; Figure 2d, short arrow) to form the calcite platelets (Figure 2d, long arrow). The exact moment of transformation from amorphous to crystalline and the detailed mechanism cannot be determined by the present experiments and is subject of further investigations. However, the electron diffraction results help to propose a remineralization mechanism:

(24) Thompson, J. B.; Paloczi, G. T.; Kindt, J. H.; Michenfelder, M.; Smith, B. L.; Stucky, G.; Morse, D.; Hansma, P. K. *Biophys. J.* **2000**, *79*, 3307.

(25) Schäffer, T. E.; Ionescu-Zanetti, C.; Proksch, R.; Fritz, M.; Walters, D. A.; Almqvist, N.; Zaremba, C. M.; Belcher, A. M.; Smith, B. L.; Stucky, G. D.; Morse, D. E.; Hansma, P. K. *Chem. Mater.* **1997**, *9*, 1731.

The circular diffraction pattern of the aggregates indicates no preferential orientation (Figure 2e), whereas that of the platelets, which bear a more smooth appearance, shows only a few diffraction peaks (Figure 1c) meaning that they consist of single crystalline domains much bigger than the nanoparticles constituting the aggregates. Considering this and the fact that the starting point is an amorphous material that can aggregate, calcite grows most presumably by mesoscale transformation here[21] (i.e., the intermediate particles directionally adhere to a growing structure and crystallize toward calcite). The shape of the aggregates indicates that they first grow in height and then fill the interstitial space. The growth in height is limited by the geometry of the matrix layers, as platelets grown on top of the outer matrix layers under the same conditions are much higher than the others (Supporting Information Figure 4). This supports a theory about natural nacre formation, where the insoluble organic matrix limits the growth of the aragonite tablets in *c*-direction.[26] The lateral growth is limited by the contact to neighboring platelets and therefore by the nucleation density, an observation also made for the natural system. Even the major difference to natural nacre, the presence of another polymorph, carries important information: it allows us to conclude that the matrix mineralization is adaptable to different crystal structures and is not restricted to a defined system.

To obtain information about the mechanical properties of the remineralized matrix, we carried out nanoindentation measurements (see Supporting Information for experimental methods and materials). Our results show that the stiffness of the samples was variable, with soft and hard regions, as is expected due to the varying degree of mineralization in different areas. Excluding the very soft regions, which consist of a mixture of embedding medium and organic matrix (with moduli < 5 GPa), we obtain a maximal value for the modulus of 37.7 GPa, with a mean value of 16.1 GPa. For comparison, measurements on nacre samples in the same geometry (transverse to the wide dimension of the mineral tablets) give a mean value of 53.6 GPa.

It is worth underlining that we used only two controlling components to retrosynthesize nacre, namely, the confining insoluble matrix and a synthetic, anionic polymer to form and stabilize the amorphous intermediate for mass transport. Absence of either the anionic polymer or the matrix results in failure to retrosynthesize the nacre structure (Supporting Information Figure 5). It remains open to prove that a third component can be used for aragonite nucleation.

It is to be concluded that amorphous precursor particles are ideal candidates for effective storage, rapid transport, and buildup of mimicked biological minerals. Only further in vivo investigations can clarify if nature uses a similar mechanism to build up biominerals. However, the results presented here suggest the possibility that biomineralization, at least nacre formation, is driven by more general physicochemical processes than commonly assumed.

Acknowledgment. We thank Dr. Miles Page for his kind scientific assistance. PD Dr. Habil Monika Fritz, Bremen, is thanked for providing the *Haliotis laevigata* shells. Financial support from DFG SPP 1117 priority program "Principles of Biomineralization" and the Max-Planck-Society are gratefully acknowledged.

Supporting Information Available: Experimental details, additional figures. This material is available free of charge via the Internet at http://pubs.acs.org.

CM052150K

(26) Belcher, A. M.; Gooch, E. E. In *Biomineralization*; Bäuerlein, E., Ed.; Wiley−VCH: Weinheim, Germany, 2000; pp 221−249.